



## Research Article

Zdeněk Šmída, Kamil Kolarčík, and Stanislav Honus\*

# Ideal mathematical model of shock compression and shock expansion

<https://doi.org/10.1515/eng-2019-0079>

Received Sep 08, 2019; accepted Oct 09, 2019

**Abstract:** Shock compression and expansion are phenomena which occur mainly in screw or vane compressors. They occur when there is an imbalance in the built-in and total pressure ratio. These are phenomena that have a negative impact on the operation of these machines and, in general, cause instability in operation, an increase in energy consumption and an overall worsening of the operational economy. The aim of this article is to present newly discovered information regarding making work processes of said compressors more effective, as in many cases, shock phenomena are subconsciously underestimated. The set aim was reached by creating an ideal simulation of isothermal compression of an ideal gas with the implementation of shock phenomena, which were performed on a screw compressor with the operating pressure 7 bar and a flow performance of  $3\,440\text{ l min}^{-1}$ . Based on the simulations performed, the hypotheses which set forth that the impact of shock phenomena ultimately leads to a sudden increase in compressor power consumption were confirmed. E.g. at 6 bar, the instantaneous power consumption increases by about 5.74% during shock compression and by about 55.95% during shock expansion. This paper deals with new insights and at the same time presents the follow-up research.

**Keywords:** Screw compressor, Built-in pressure ratio, Shock compression, Shock expansion, Mathematical model

**\*Corresponding Author: Stanislav Honus:** VŠB – Technical University of Ostrava, Faculty of Mechanical Engineering, Department of Energy Engineering, 17. listopadu 2172/15, 708 00 Ostrava – Poruba, Czech Republic; VŠB – Technical University of Ostrava, Centre ENET, 17. listopadu 2172/15, 708 00 Ostrava – Poruba, Czech Republic; Email: stanislav.honus@vsb.cz

**Zdeněk Šmída:** VŠB – Technical University of Ostrava, Faculty of Mechanical Engineering, Department of Energy Engineering, 17. listopadu 2172/15, 708 00 Ostrava – Poruba, Czech Republic; Email: zdenek.smida@vsb.cz

**Kamil Kolarčík:** VŠB – Technical University of Ostrava, Faculty of Mechanical Engineering, Department of Energy Engineering, 17.

## 1 Introduction

The production of compressed air or other technical gases is an integral part of modern industry. This is a very energy-intensive process, with 10 to 30% of the world's total electricity consumed [1]. Given the fact that electricity consumption in society is showing steady growth [2], the trend at present is to look for possible savings even in applications that have not been to this day characterized by significant “losses” of electricity [1–3].

An analysis of ten years of operation of a typical air compressor published in [4] has shown that electricity costs account for approximately 76% of total operating expenditure, while maintenance and spare parts form only a quarter of expenses, see Appendix A. The operator should therefore make an effort to operate the compressor as efficiently as possible to reduce these costs.

This is because during the working process of the compressor there are a number of thermodynamic changes that depend not only on the physical properties of the working medium and the nature of the ongoing state change, but also on the conditions outside the compressor, eg technical condition of the compressor unit and piping system [5, 6]. The external conditions are not stable during the actual operation of the compressor and their changes may, under certain circumstances, adversely affect the compression process itself, and may produce negative operational phenomena known as shock compression or shock expansion [7–11].

Several authors have been involved in the study of shock compression and shock expansion, for example: Jaroslav Kaminský and Kamil Kolarčík described the principle of the function of shock phenomena in terms of thermodynamics of displacement compressors and defined the working space utilization factor  $l_{sc}$  for screw compressors, as an important parameter for defining the actual flow performance of the machine [6, 15]. Jeffrey R. LaPlante speaks of shock expansion as a process that has

listopadu 2172/15, 708 00 Ostrava – Poruba, Czech Republic; Email: kamil.kolarcik@vsb.cz



a much higher impact on work process efficiency than shock compression, because in shock compression, the specific loss work only concerns the overpressure of the gas backflow. However, in terms of shock expansion, there is a thwarting of the specific work for the entire volume of transported gas [12]. In his article, Jurgen Wennermar mentions, *inter alia*, that: “internal overheating occurs during shock expansion”. The compressed and transported gas also has the function of a coolant which dissipates some of the compression heat. In the event that the shock expansion removes a significantly large amount of gas and possibly even oil from the working space, compression heat isn’t conducted away sufficiently. According to the article, this problem can occur especially when starting already heated compressors with built-in volume ratio  $\gamma > 2.5$  [-] [13]. Huang Paul Xiubao discusses whether shock events can be considered as “isochoric” state changes or rather those that are inherent to irreversible adiabatic state changes. He gives examples based on the operation of the Roots blower [14]. The same author together *et al.* in further studying the gas pulsation, designed and developed a pulse trap method to reduce gas flow ripple and reduce noise during the process [16]. H. Wu *et al.* created a theoretical and experimental study of the turbulence of compressed air at the discharge of a screw compressor under various discharge gas conditions [17]. Mujic *et al.* focus on the shape of the discharge port. They concluded that optimizing the shape of the discharge port significantly affects the amplitude and intensity of gas pulsations at the screw compressor discharge [18].

These articles first defined the shock phenomena theoretically and then formed the basis for further research of shock phenomena such as the creation of CFD simulations of these phenomena. So far, the theoretical knowledge outweighs the practical knowledge.

The aim of the first phase of the research presented in this article is to support this knowledge with calculated data of changes in specific compression work and changes in isothermal power input of a screw compressor obtained from a mathematical computational model. The model described in this paper can easily be modified and replaced with initial conditions for various situations and respective screw compressors, which makes it suitable for comparing results and especially for further research. The trend of the results presented in this article is experimentally verified. The content of this article is both an analysis of computational methods used for the creation of a mathematical model, as well as an evaluation of results and discussion of possible further steps in researching shock phenomena.

## 2 Methods

### 2.1 Theoretical Background of Shock Compression and Shock Expansion

Shock Compression or Under Compression (UC) occurs when the built-in pressure ratio  $\pi$  [-] is less than the total pressure ratio  $\sigma$  [-] of a connected piping system, or pressure capability of the compressor, is lower than the gas pressure in the piping system  $p_D$  [Pa]. Ideally, the theoretical process of the process is shown in Figure 1(a), wherein the figure represents only a schematic representation and is not shown on a real scale.

The gas is first isothermally compressed from the pressure at suction point  $p_1$  [Pa] to the pressure at the compressor outlet point  $p_2$  [Pa], which is however lower than the piping system pressure  $p_D$  [Pa]. When the workspace is connected to the discharge port, there is an instant shock compression to pressure  $p_D$  [Pa]. Shock compression is considered an isochoric state change in this ideal transformation event.

The higher pressure gas from the piping system is pushed back into the compressor unit or into the working space, generally into the area with lower pressure. The compressor drive must do extra work to overcome this reverse gas flow. This action can also manifest itself in greater axial forces acting on the bearings. At the same time, in the reverse flow, the returning gas can transfer part of its enthalpy to the gas that has been compressed so far, and this can lead to an increase in the temperature of the compressed gas. Shock compression generally results in an increase in compression work and compressor power consumption, and in an increase in operating and service costs for operating the compressor unit. The shaded area represents an overall increase in compression work  $A_{ztr}$  [J] [6, 19–22].

Shock Expansion or Over Compression (OC) occurs when the built-in pressure ratio  $\pi$  [-] is greater than the total pressure ratio  $\sigma$  [-] of a connected piping system, or the compressive capacity of the compressor is higher than the gas pressure in the piping system  $p_D$  [Pa].

The gas is first isothermally compressed from the suction point pressure  $p_1$  [Pa] to the pressure at the compressor outlet  $p_2$  [Pa], which is higher than the piping system pressure  $p_D$  [Pa]. As soon as the working space is connected to the discharge port, the gas immediately expands from the pressure  $p_2$  [Pa] to pressure  $p_D$  [Pa].

The compressor in this case compresses the gas to an “unnecessarily” high pressure. Therefore, more compression work is needed to compress to a higher pressure. In-

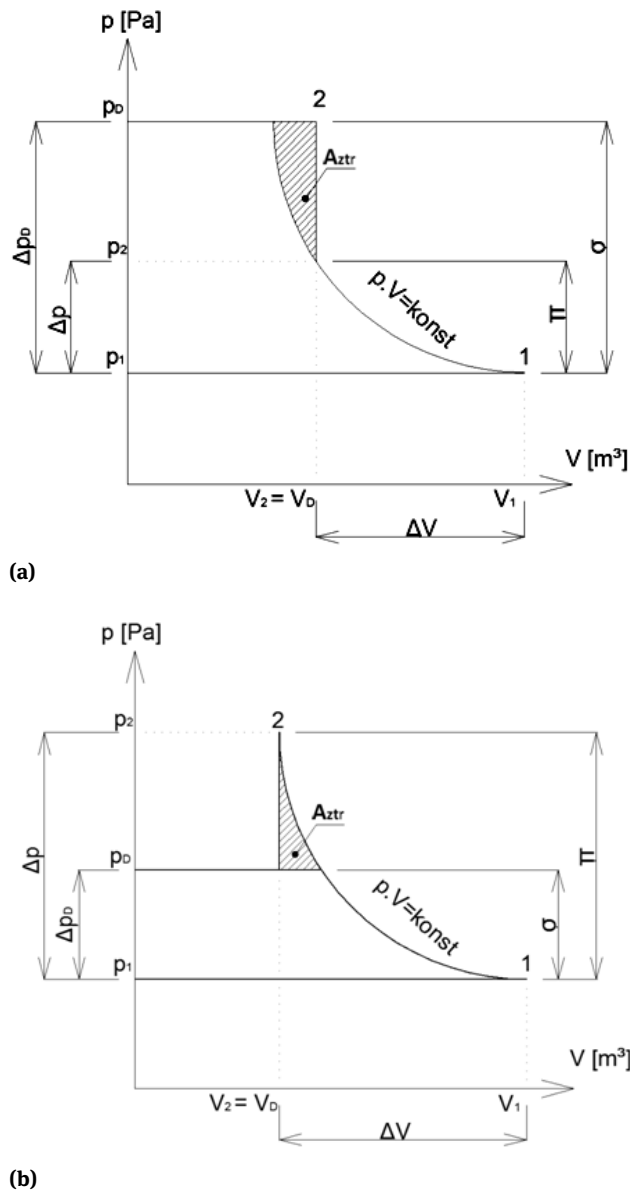


**Figure 1:** Ideal indicator  $p$ - $V$  diagram of shock compression (a) and shock expansion (b)

creasing the compression is working at a loss  $A_{ztr}$  [J] the amount of which is proportional to the shaded area shown in Figure 1(b).

Shock expansion is also a negative phenomenon that manifests itself in pressure pulses that emit into an “empty” discharge line, and these pulses can, under certain conditions, damage equipment on the discharge side of the compressor. Ultimately, the gas is compressed to “unnecessarily” high pressure, requiring more compression work and more power consumption, which will result in a worsened economy of compressor operation [6, 19–22].

## 2.2 An ideal mathematical model of the screw compressor process with shock phenomena & Experimentals

### 2.2.1 Ideal mathematical model

The ideal mathematical model is a system of equations that consists in simulating the working process of a screw compressor with the implementation of shock compression and shock expansion at various intensities of pressure pulses.

The input values for working process calculation listed in Table 1 contain two kinds of parameters. These are basic physical constants and data taken from the data sheet of the selected screw compressor, see datasheet [23]. The criterion for selecting the simulated screw compressor was the technical data sheet with the following parameters: actual compressor flow performance  $\dot{V}_d$  [l min<sup>-1</sup>], main rotor speed  $n_H$  [min<sup>-1</sup>] (nominal speed of compressor), the number of teeth of the main rotor  $z_H$  [-] and installed electric motor power output  $P_{V,el}$  [kW]. It therefore isn't dependent on the manufacturer or the design of the compressor, because the ideal mathematical model is primarily used to calculate changes in specific compression work and isothermal power consumption of the compressor, ie to quantify phenomena subject to basic physical laws and principles that are common to all compressors of a given type.

The ideal mathematical model works with several idealizations. The working medium is considered to be air with properties that correspond to the ideal gas. The real working process is replaced by ideal isothermal compression. The impact of the intake gas humidity on the working process is taken into account in implementing the relative air humidity into the task.

### 2.2.2 Calculation of working process

First, the working process of the simulated screw compressor was calculated for further simulation needs. First in the analysis was the calculation of mass flow performance  $\dot{m}_d$  [kg·s<sup>-1</sup>], theoretical flow performance  $\dot{V}_t$  [m<sup>3</sup>·s<sup>-1</sup>] and the actual power consumption of the compressor  $P_{p,c}$  [kW]. Based on the knowledge of these quantities, the ideal specific isothermal technical compression work will then be calculated  $a_{t,it}$  [J·kg<sup>-1</sup>] necessary to compress the gas of a given initial condition to the required compressor discharge pressure, see equation (1) [27, 28, 33].

$$a_{t,it} = r_{air} \cdot T \cdot \ln(\sigma) \quad (1)$$

Table 1: Input values of ideal mathematical model

Name of quantity	Quantity	Value	Unit
Absolute compressor suction pressure - <i>selected</i>	$p_1$	1	Bar
Intake air temperature - <i>selected</i>	$t_1$	15	°C
(Limit) Relative Humidity - <i>selected</i>	$\varphi$	80	%
Water vapor specific gas constant [24]	$r_w$	461.5	$\text{J}\cdot\text{kg}^{-1}\cdot\text{K}^{-1}$
Saturated water vapor partial pressure [24]	$p''$	1.704	Bar
Absolute compressor discharge pressure [24]	$p_2$	7	Bar
Working space utilization factor at nominal speed	$\lambda$	0.644	-
Actual compressor flow performance [23]	$\dot{V}_d$	3 440	$\text{l}\cdot\text{min}^{-1}$
Main rotor (compressor) speed [23]	$n_H$	6 250	$\text{min}^{-1}$
Number of main rotor teeth [23]	$z_H$	5	-
Installed motor power [23]	$P_{V,el}$	22	kW
Belt drive efficiency [25]	$\eta_{BG}$	96.5	%
Compressibility factor - <i>selected</i>	$z$	1	-

Table 2: Simulated screw compressor working process table

$p_2$ [bar]	$\sigma_c$ [-]	$\lambda$ [-]	$\dot{V}_d$ [ $\text{l}\cdot\text{min}^{-1}$ ]	$\dot{m}_d$ [ $\text{kg}\cdot\text{s}^{-1}$ ]	$a_{t,it}$ [ $\text{kJ}\cdot\text{kg}^{-1}$ ]	$P_{it}$ [kW]	$P_{p,vn}$ [kW]	$\eta_{it}$ [%]	$c$ [ $\text{kWh}\cdot\text{m}^{-3}$ ]
1	1	0.78	4166	0.0835	0	0	4.01	50.1	0.016
2	2	0.76	4081	0.0818	57.6	4.71	11.55	50.8	0.038
3	3	0.74	3953	0.0793	91.3	7.27	15.53	51.2	0.060
4	4	0.72	3825	0.0767	115.2	8.93	18.59	51.6	0.075
5	5	0.69	3696	0.0741	133.8	9.80	19.95	52.1	0.086
6	6	0.67	3568	0.0715	148.9	10.59	20.39	52.4	0.095
7	7	0.64	3440	0.0690	161.8	11.16	21.23	52.6	0.103
8	8	0.62	3312	0.0664	172.9	11.56	22.50	52.0	0.111
9	9	0.60	3184	0.0638	182.7	11.63	23.86	50.5	0.121
10	10	0.57	3055	0.0613	191.4	11.58	27.80	49.0	0.131

Equation (1) symbols explanation:  $r_{air}$  [ $\text{J}\cdot\text{kg}^{-1}\cdot\text{K}^{-1}$ ] specific gas constant of air,  $T$  [K] thermodynamic temperature (general notation),  $\sigma$  [-] pressure ratio (general compression notation).

The nominal pressure ratio used as the reference point to be used for the shock phenomena implementation  $\sigma_c = 7$  calculated on the basis of the specified absolute pressure at the compressor discharge  $p_2$  (ie  $\sigma_c = p_2/p_1$ ). The reference point corresponds to the nominal parameters from the compressor datasheet [23]. The reference point row is color coded in Table 2 below. The calculation was first performed for a range of absolute compressor discharge pressures from 1 to 10 [bar]. The upper limit corresponds to the pressure at which the safety valve opens in the simulated

compressor as described in the datasheet [23]. At the same time, this limit allows for a wider range of shock phenomena simulation because the line pressure is specified by the operating pressure  $p_2$ .

Thereafter, the model task was expanded by an additional 3 [bar] on the displacement for the purpose of simulation and calculation only, due to extrapolation of the calculation and prediction of further development of calculated quantities. Another important parameter is the working space utilization factor  $\lambda$  [-] the value of which was determined from literature data [6], see Figure 2.

The nominal total pressure ratio  $\sigma_c$  that is necessary for determining  $\lambda$  was calculated as  $\sigma_c = p_2/p_1$ . The nominal rotational speed  $n$  was read from the simulated com-

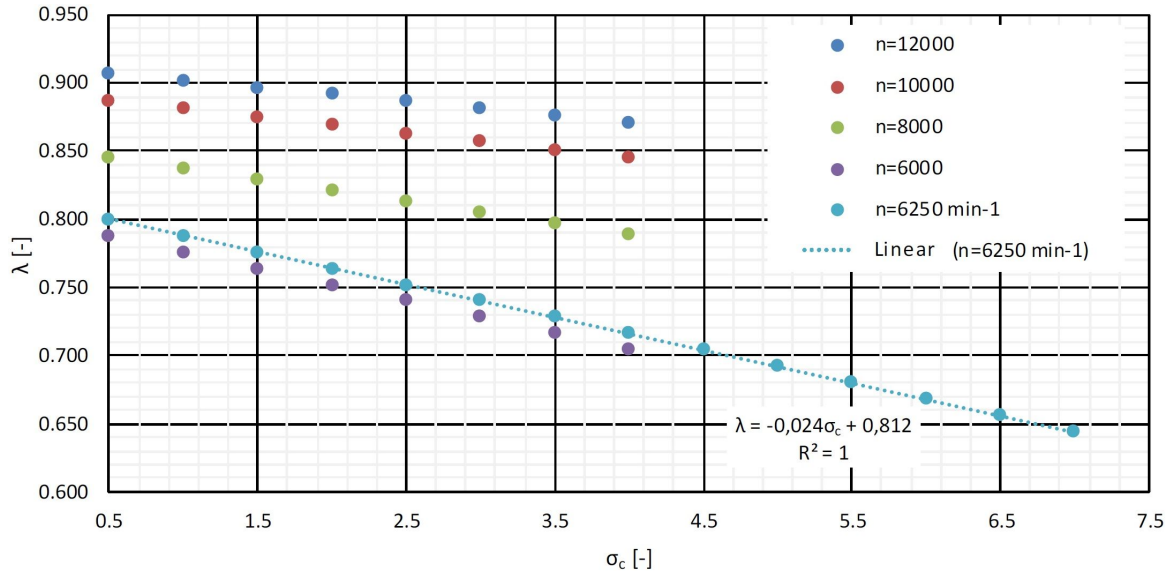


Figure 2: Dependence  $\lambda$  on speed and total pressure ratio

pressor datasheet [23]. The diagram in [6] was designed for maximum total pressure ratio  $\sigma_c = 4$  [-] and only selected compressor speed lines. For this reason, linear interpolation and linear extrapolation of the working space utilization factor relative to the total pressure ratio and the speed were performed. The result of this partial calculation is the value of the nominal utilization factor of the working space  $\lambda = 0.644$  [-] for the nominal compressor flow performance  $\dot{V}_d = 3\,440$  [ $\text{min}^{-1}$ ].

From the calculation of the slope of the line of the nominal rotation speed  $n_H = 6\,250$  [ $\text{min}^{-1}$ ], see equation (2), with decreasing total pressure ratio  $\sigma_c$  the value of the working space utilization factor  $\lambda$  increases and vice versa. As the pressure ratio increases, the pressure difference between the working chambers increases and this results in an increase in internal leaks [6]. According to equation (2) for different the total pressure ratio  $\sigma_c$  [-] there were the working space utilization factor  $\lambda$  [-] determined for the other rows of Table 2.

$$\begin{aligned} \lambda &= (-0.084/3.5) \cdot \sigma_c + (2.842/3.5) \\ &= -0.024 \cdot \sigma_c + 0.812 \end{aligned} \quad (2)$$

An essential quantity in Table 2 is the ideal isothermal efficiency  $\eta_{it}$ . Nominal isothermal efficiency  $\eta_{it,n} = 52.55$  [%] was calculated on the basis of the isothermal power consumption  $P_{it}$  [kW], the internal compressor power consumption  $P_{p,vn}$  [kW] or on the basis the installed power of the electric motor  $P_{V,el}$  [kW], belt drive efficiency  $\eta_{BG} = 96.5$  [%], mass flow performance  $\dot{m}_d$  [ $\text{kg}\cdot\text{s}^{-1}$ ] and specific isothermal compression work  $a_{t,it}$  [ $\text{J}\cdot\text{kg}^{-1}$ ] from equa-

tion (3) [19].

$$\eta_{it} = P_{it}/P_{p,vn} = (\dot{m}_d \cdot a_{t,it})/(P_{V,el} \cdot \eta_{BG}) \quad (3)$$

Based on the fact that at the reference point, at nominal operating quantities (*i.e.*  $\pi = \sigma_c = 7$ ) the equipment should be operated with the highest efficiency (so that its operation is as convenient and economical as possible), other efficiencies were determined by extrapolation based on numerical and geometrical (shape) similarity to the calculated energy efficiency with actual efficiency characteristic generated from the results of operational measurements of screw compressors, see Appendix B.

Practical data were obtained from operational measurements of screw compressors in commercial companies. The single-stage screw compressor from measurement No. 1 had the following rated parameters in the datasheet  $\dot{V}_d = 1\,540$  [ $\text{m}^3\cdot\text{h}^{-1}$ ],  $\sigma_c = \pi = 7$  [-] and  $P_{P,el} = 164$  [kW]. The screw compressor from measurement No. 2 had the following nominal parameters stated in the datasheet  $\dot{V}_d = 6\,500$  [ $\text{m}^3\cdot\text{h}^{-1}$ ],  $\sigma_c = \pi = 8.5$  [-] and  $P_{P,el} = 850$  [kW]. The calculation methodology is based on the formulas in [6].

The absolute compressor discharge pressure  $p_{2}$  has been entered, see Table 1. Quantities  $\sigma_c$  [-],  $\dot{V}_d$  [ $\text{l}\cdot\text{min}^{-1}$ ],  $\dot{m}_d$  [ $\text{kg}\cdot\text{s}^{-1}$ ],  $a_{t,it}$  [ $\text{kJ}\cdot\text{kg}^{-1}$ ],  $P_{it}$  [kW] and  $c$  [ $\text{kWh}\cdot\text{m}^{-3}$ ], shown in Table 2, were calculated based on the equations given, eg in the literature [28] and [29]. The working space utilization factor  $\lambda$  [-] was determined according to the original equation (2), and isothermal efficiency  $\eta_{it}$  [-] with subsequent internal compressor power consumptions  $P_{p,vn}$  [kW] in non-nominal operating states were determined on



the basis of experimentally measured data from operating measurements of screw compressors.

The results shown in Table 2 are graphically represented by the energy characteristic curves of “Simulations” in Appendix B. With increasing compressor discharge pressure  $p_2$  the total pressure ratio increases  $\sigma_c$ , which translates into a decrease in the working space utilization factor  $\lambda$ . Actual compressor flow performance  $\dot{V}_d$  and the compressor mass flow performance  $\dot{m}_d$  decreases along with a decreasing coefficient of utilization of working space. Conversely, with increasing outlet pressure  $p_2$  there is an increase in the required specific isothermal compression work  $a_{t,it}$ , isothermal power consumption  $P_{it}$  and internal power consumption of the screw compressor  $P_{p,vn}$ . Isothermal efficiency of the compressor  $\eta_{it}$  was simulated so that the local maximum of this quantity is at the nominal total pressure ratio, which is also the in-built pressure ratio  $\sigma_c = \pi$ . Specific energy consumption  $c$  in nominal operating condition corresponds to the optimum specific consumption value for screw compressors,  $c_{sc,opt} \cong 0.1$  [kWh·m<sup>-3</sup>] [29].

### 2.2.3 Checking the correctness of the ideal mathematical model

The ideal mathematical model was created as a combination of equations taken from literature and original data (measured values) obtained from the measurement of screw compressors. Therefore, it was necessary to check the accuracy of the created simulation. The verification of the calculated values was performed based on the geometric and numerical similarity of the calculated energy characteristics obtained from the calculation of mathematical equations and the measured energy characteristics of the screw compressors given in Appendix B.

As shown in Appendix B: In general, the trends of the regression curves generated from the calculations correspond to the trends of the actual energy characteristics obtained from operational measurements. The different tendency of the energy characteristics is due to the comparison of screw compressors with different flow performance parameters  $\dot{V}_{d,S} = 206.4$  [m<sup>3</sup>·h<sup>-1</sup>],  $\dot{V}_{d,M1} = 1\,540$  [m<sup>3</sup>·h<sup>-1</sup>] and  $\dot{V}_{d,M2} = 6\,500$  [m<sup>3</sup>·h<sup>-1</sup>] and power consumption  $P_{p,el,S} = 23$  [kW],  $P_{p,el,M1} = 164$  [kW] and  $P_{p,el,M2} = 850$  [kW] [7, 24].

- **Appendix B - Pressure characteristics** - The graph shows a clear trend of increasing compressor performance  $\dot{V}_d$  with decreasing overall pressure ratio  $\sigma_c$ .

- **Appendix B - Power consumption characteristics** - Displacement compressors have, compared to dynamic compressors, a negative slope of the input characteristics, ie. with increasing compressor flow performance  $\dot{V}_d$ , its power consumption decreases  $P_{p,el}$ .
- **Appendix B - Efficiency characteristics** - Compressor efficiency has a distinct local extreme representing the operating state with the highest efficiency when the machine flow performance changes  $\dot{V}_d$ , either in terms of its rise or fall, and the isothermal efficiency of the compressor  $\eta_{it}$  will always fall.
- **Appendix B - Specific energy consumption characteristics** - Specific compressor power consumption  $c$  decreases as its flow performance increases  $\dot{V}_d$ .

Thus, the correctness of the computational procedure of the ideal mathematical model was verified by comparing the shape of the calculated and measured curves and the impact analysis itself could be approached.

### 2.2.4 Shock phenomena and their integration into the compressor working process

The working process of an ideal screw compressor would account for thermodynamic calculation of the isothermal state change, which is the ideal transformation of the ideal gas state applied to a displacement screw compressor [19]. In the case of an isothermal state change, the value of the general polytropic exponent is equal to one  $n_{it} = 1$ . In this process, it was therefore assumed that all the heat generated during compression would be removed by cooling outside the compressor working space [24, 28, 30, 33].

The above shown Figure 3 is a comprehensive graphical representation of a screw compressor working process simulation. It is an indicator  $p$ - $v$  diagram showing curves representing isothermal, isentropic and isochoric state change. These curves are mathematically written by the equations of isotherms (4), isentrops (5) and isochors (6) [24, 28, 31, 32].

$$p \cdot v^1 = p \cdot v = \text{const.} \quad (4)$$

$$p \cdot v^\kappa = \text{const.} \quad (5)$$

$$p \cdot v^\infty = p^{1/\infty} \cdot v = v = \text{const.} \quad (6)$$

Equations (4), (5) and (6) symbols explanation:  $p$  [Pa] pressure,  $v$  [m<sup>3</sup>·kg<sup>-1</sup>] specific volume,  $\kappa$  [-] Isoentropic exponent - Poisson's constant.

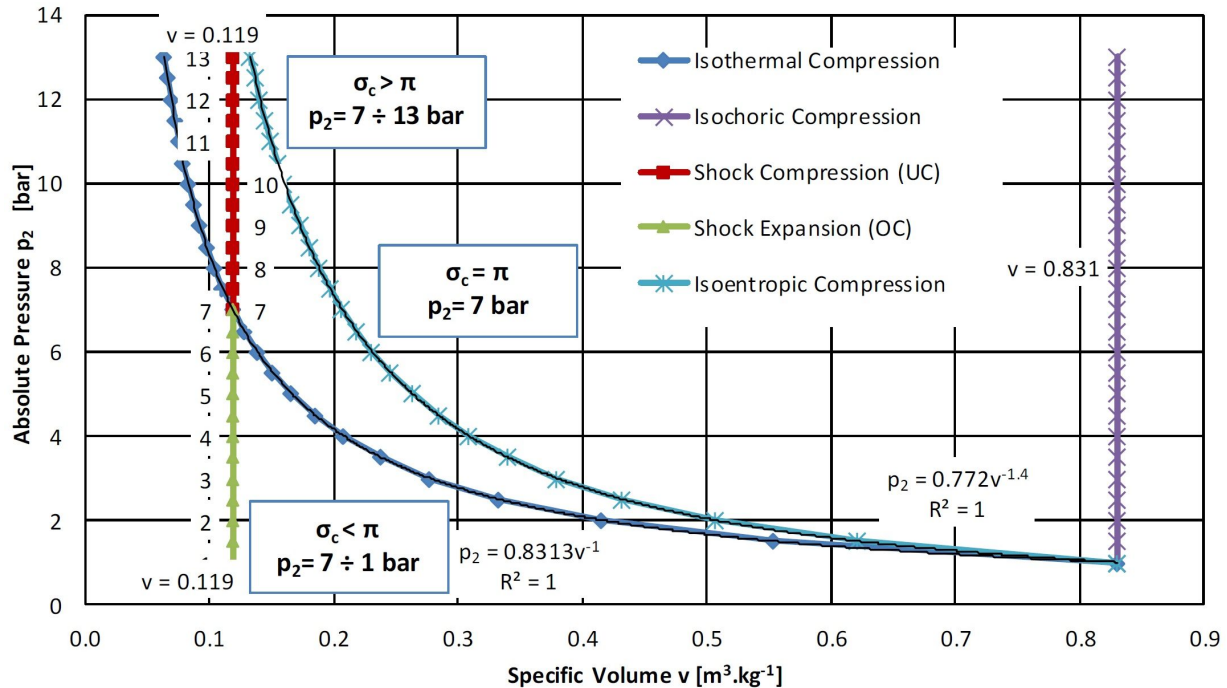


**Figure 3:** Indicator p-v diagram of the ideal working process of a screw compressor with the implementation of shock phenomena graphically describing thermodynamic processes in a mathematical model

Isothermal state change ( $p_2 = 0.8313 \cdot v^{-1}$ ) describes the working process of a simulated ideal screw compressor. Isentropic state change ( $p_2 = 0.772 \cdot v^{-1.4}$ ) with a polytropic exponent corresponding to the Poisson constant  $n_{ize} = \kappa$  is presented here mainly because of its symbolism. Along with the isothermal state change, isentropic change represents the boundary, or marginal, energy transformation points between which the actual working processes take place [24].

In the literature [6, 12, 13], the shock compression and shock expansion diagrams are depicted primarily as isochoric or very close to this state change. For this reason, this variant was also chosen for the ideal mathematical model. The polytropic exponent value in this case is equal to infinity  $n_{izch} = \infty$ . This idealization is based on the fact that shock compression or shock expansion are very fast-acting phenomena, and at a constant volume, there is almost a step change in gas pressure. Curves, respectively the shock compression and shock expansion lines are mathematically represented by equation (6). In the diagram of Figure 3, in order to compare the amounts of compression work need, there were isochora generated for the whole pressure ratio range ( $v = 0.831$ ) [28].

The shock phenomena in Figure 3 are derived from the reference point with the coordinate  $p_2 = \pi = \sigma_c = 7$ . Where, shock compression  $\pi < \sigma_c$  occurs when a shock phenomenon takes place on a straight line ( $v = 0,119$ ) and

shock expansion  $\sigma_c > \pi$  occurs when the process runs in a straight line of the same equation of the line perpendicular with the horizontal axis “x”, respectively “v” ( $v = 0,119$ ).

## 2.2.5 Calculation methodology

The calculation methodology is based on the principle of the indicator p-v the diagram, see Figure 3 and at the equations for the calculation of the specific compression (technical) isothermal work  $a_{t,it}^\pi$  and the specific compression (technical) work  $a_{t,izch}^\pi$ . In general, the calculation methodology is based on literature [24].

Equations (7) and (8) are specific compression works for isothermal  $a_{t,it}^\pi$  and isochoric state change  $a_{t,izch}^\pi$  wherein the works are related to a reference line having a built-in pressure ratio  $\pi$ , whose value is constant for the simulated screw compressor and therefore the value of the mentioned works does not change either.

$$a_{t,it}^\pi = r_{air} \cdot T \cdot \ln(\pi) \quad (7)$$

$$a_{t,izch}^\pi = v_\pi \cdot (p_2 - p_1) \quad (8)$$

Equations (7) and (8) additional symbols explanation:  $r_{air}$  [ $J \cdot kg^{-1} \cdot K^{-1}$ ],  $T$  [K] thermodynamic temperature (general notation),  $\pi$  [-] built-in pressure ratio,  $v_\pi$  [ $m^3 \cdot kg^{-1}$ ]

specific volume at built-in pressure ratio (the same parameter in the equation (10)),  $p_2$  [Pa] absolute compressor discharge pressure (operating pressure) and  $p_1$  [Pa] absolute compressor intake pressure.

Equations (9) and (10) are also specific compression works for isothermal  $a_{t,it}^{\sigma_c}$  and isochoric  $a_{t,izch}^{\sigma_c}$  state change but in this case their size is always related to the particular network pressure  $p_D$ , respectively to the total pressure ratio  $\sigma_c$ , which depends on the intensity of the impact  $I_r$ .

$$a_{t,it}^{\sigma_c} = r_{air} \cdot T \cdot \ln(\sigma_c) \quad (9)$$

$$a_{t,izch}^{\sigma_c} = v_{\pi} \cdot (p_D - p_1) \quad (10)$$

Equation (11) represents the difference in changes in specific isothermal and isochoric compression work  $\Delta a_{UC}$ . This is an increase in work due to shock compression. Equation (12) represents the same situation, but for shock expansion  $\Delta a_{OC}$ .

$$\begin{aligned} \Delta a_{UC} &= \Delta a_{t,izch} - \Delta a_{t,it} \\ &= (a_{t,izch}^{\sigma_c} - a_{t,izch}^{\pi}) - (a_{t,it}^{\sigma_c} - a_{t,it}^{\pi}) \end{aligned} \quad (11)$$

$$\begin{aligned} \Delta a_{OC} &= \Delta a_{t,it} - \Delta a_{t,izch} \\ &= (a_{t,it}^{\pi} - a_{t,it}^{\sigma_c}) - (a_{t,izch}^{\pi} - a_{t,izch}^{\sigma_c}) \end{aligned} \quad (12)$$

An increase in specific compression work during shock compression  $a_{t,it,UC}$  is calculated with equation (13) and the lost specific compression work during shock expansion  $a_{t,it,OC}$  with equation (16). The immediate isothermal power consumption required to compress the ideal gas during shock compression  $P_{it,UC}^{\sigma_c}$  for a given total pressure ratio  $\sigma_c$ , therefore shock intensity  $I_r$  is calculated with equation (14), for shock expansion a similar quantity is determined from equation (17). Desired change of instantaneous isothermal power consumption during shock compression  $\Delta P_{it,UC}$  is found from equation (15) and in the case of shock expansion  $\Delta P_{it,OC}$  it is equation (18).

$$a_{t,it,UC} = a_{t,it}^{\sigma_c} + \Delta a_{UC} \quad (13)$$

$$P_{it,UC}^{\sigma_c} = \dot{m}_d \cdot a_{t,it,UC} \quad (14)$$

$$\Delta P_{it,UC} = P_{it,UC}^{\sigma_c} - P_{it}^{\pi} \quad (15)$$

$$a_{t,it,OC} = a_{t,it}^{\sigma_c} + \Delta a_{OC} \quad (16)$$

$$P_{it,OC}^{\sigma_c} = \dot{m}_d \cdot a_{t,it,OC} \quad (17)$$

$$\Delta P_{it,OC} = P_{it}^{\pi} - P_{it,OC}^{\sigma_c} \quad (18)$$

The reason for a change of a power consumption is the direct connection of the necessary specific compression work to the required instantaneous power consumption of the compressor. See equation (19) that is the product of a quantity  $\dot{m}_d$  [kg·s<sup>-1</sup>] mass flow performance and a quality  $a_{t,it}$  [J·kg<sup>-1</sup>] ideal specific isothermal technical compression work [6].

$$P_{it} = \dot{m}_d \cdot a_{t,it} \quad (19)$$

### 3 Results

The available literature [6, 12, 13] show that shock compression and shock expansion have a so far unquantified negative impact on the required compression work and instantaneous power consumption of the compressor. The ideal mathematical model assumption shown in Figure 1 confirmed and supplied a numerical evaluation that is in accordance with the input values of the calculation from Table 1.

The Figure 4 presents an evaluation of the calculation of the increase (change) of the required specific compression work during shock compression  $\Delta a_{UC}$  [%] and shock expansion  $\Delta a_{OC}$  [%], see equations (7–12). The calculation was relative to the reference line at each step. Thus, the intensity of the pressure pulse, or shock (compression or expansion) wave, was changed  $I_r$ .

A compression wave is an aperiodic nonlinear physical phenomenon, in which the environment spreads in the form of an almost step change in physical quantities describing the environment. Expansion waves, on the other hand, represent dilution of the environment. Both of these phenomena are described in Hugoniot's theorem, which characterizes gas flow behavior as a function of its velocity [9].

From the results in Figure 4 it is clearly evident that the value of the increase in the specific compression work required increases with the increasing intensity of the shock process. The increase of the work has an exponential character in the case of shock compression and shock expansion. The growth trend along with the equation is given in Figure 4. The Figure 5 directly follows the previous figure with the results of the power consumption changes.



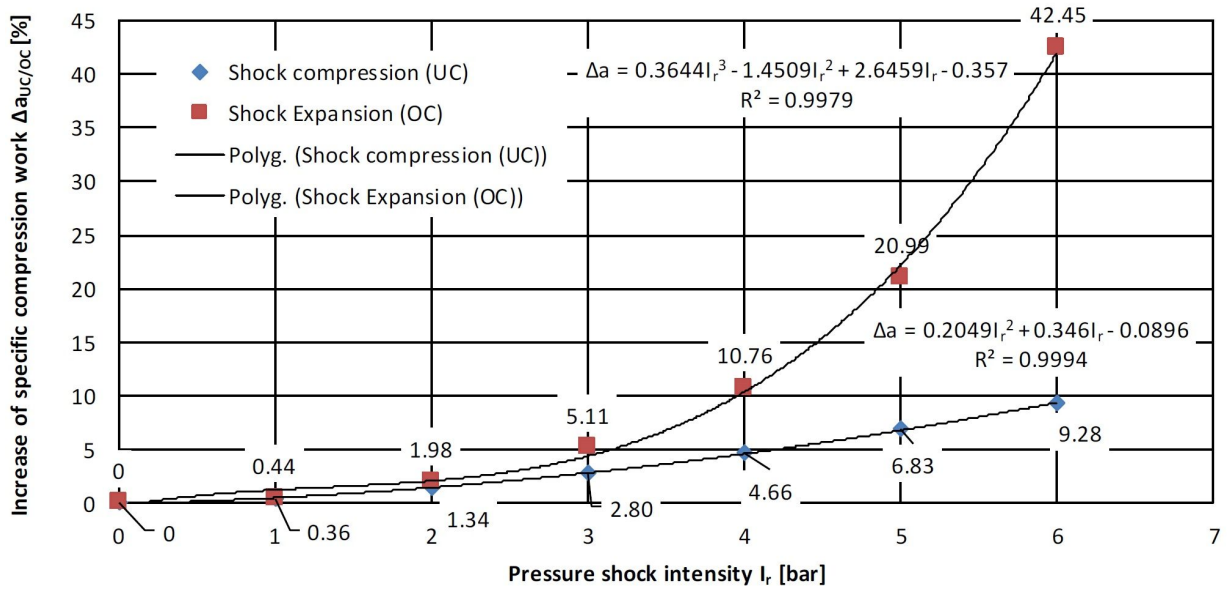


Figure 4: Diagram of increase (change) of specific compression work needed to compress ideal gas in dependence on the intensity of the Shock compression (UC) and the Shock expansion (OC)

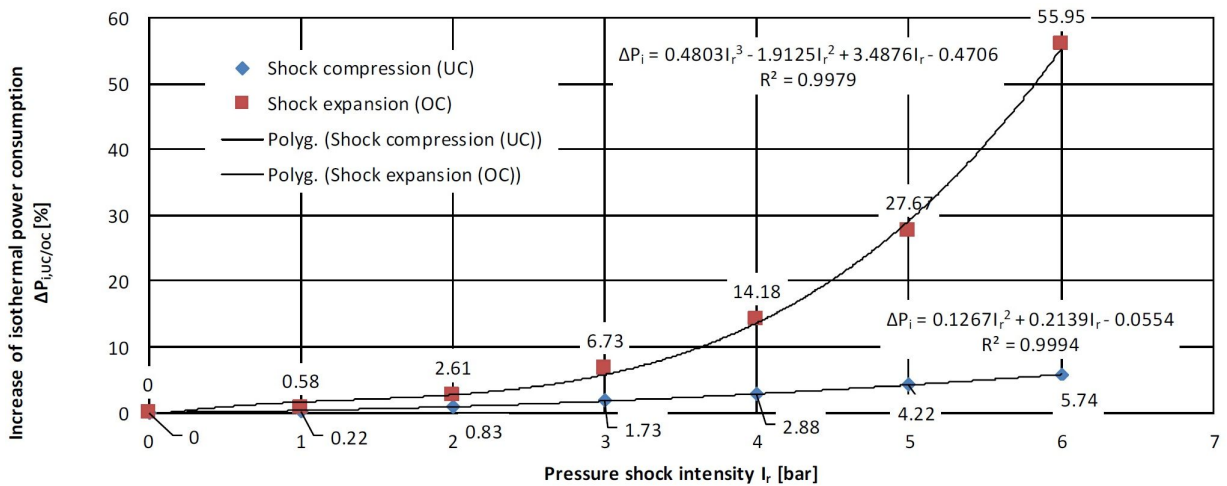


Figure 5: Diagram of increase (change) of instantaneous isothermal power consumption needed for compression in dependence of shock compression (UC) and shock expansion (OC) intensity

### 4 Discussion

The reason for the much greater increase in the required specific compression work and the required instantaneous power consumption during shock expansion is that the shock expansion generally causes the gas to be compressed to a greater pressure than at that specific point in the piping system. This means that in the case of a pressure pulse, which will result in pressure equalization, the already invested compression work will be lost. On the other hand in shock compression, there is a real increase in the necessary specific compression work, which must be sup-

plied to the compressor in order to overcome, above all, the effect of the reverse flow of higher pressure gas back to the compressor unit. In this case it is therefore necessary to increase the input energy due to the partial dissipation of the energy caused by the shock wave [9].

The reason for the much greater increase in the required specific compression work and the required instantaneous power consumption during shock expansion is that the shock expansion generally causes the gas to be compressed to a greater pressure than at that specific point in the piping system. This means that in the case of a pressure pulse, which will result in pressure equalization, the

already invested compression work will be lost. On the other hand, in shock compression, there is a real increase in the necessary specific compression work, which must be supplied to the compressor in order to overcome, above all, the effect of the reverse flow of higher pressure gas back to the compressor unit. In this case it is therefore necessary to increase the input energy due to the partial dissipation of the energy caused by the shock wave [9].

With increasing pressure pulse intensity, both in shock compression and shock expansion, there is an exponential increase in the required instantaneous compressor power consumption.

## 5 Conclusion

This paper dealt with problems of negative phenomena occurring in operation of positive displacement compressors with built-in pressure ratio. It is an issue that is not much discussed in professional circles, and therefore one of the main objectives of this research is to supplement the existing theoretical knowledge with calculated data, namely the quantification of the necessary compression work and the instantaneous power consumption required to compress gas during the shock compression and shock expansion. The aim of the ideal mathematical model was to prove the theoretical assumptions known from the available technical literature and scholarly articles based on the application of mathematical-physical equations and the theory of displacement compressors.

On the basis of the calculations, it was found and verified that the instantaneous isothermal power consumption required to compress the ideal gas, which the ideal machine draws during shock compression or shock expansion, is greater than the instantaneous isothermal power consumption to be supplied to the compressor in a stable state without any impact of shock phenomena, eg:

In order for the simulated screw compressor to compress the ideal gas to a built-in pressure ratio  $\pi = \sigma_c = 7$  [-], it needs to supply the machine with the nominal isothermal compression work calculated by  $a_{t,it} = 161.759$  [kJ·kg<sup>-1</sup>] and nominal isothermal power consumption  $P_{it} = 11.157$  [kW]. In the case of the shock compression with the pressure pulse intensity  $I_r = 6$  [bar], that is, when the pressure is compressed to the total pressure ratio  $\sigma_c = 13$  [-] the specific isothermal compression work will increase to value  $a_{t,it,UC} = 171.042$  [kJ·kg<sup>-1</sup>], i.e. to the specific isothermal compression work by 9.28 [%] of the nominal work. At the same time, the isothermal power consumption increases  $P_{it,UC} = 11.797$  [kW], ie an increase of 5.74 [%] of the

nominal power consumption. In the event of a sudden expansion of the same pressure pulse intensity  $I_r = 6$  [bar], ie, the shock expansion to the total pressure ratio  $\sigma_c = 1$  [-], the specific isothermal compression work lost is of the value  $a_{t,it,OC} = 252.265$  [kJ·kg<sup>-1</sup>], i.e. thwarting 42.45 [%] of the nominal work. In terms of isothermal power consumption, it is a waste of power consumption value  $P_{it,OC} = 17.339$  [kW], work lost is of the value  $a_{t,it,OC} = 252.265$  [kJ·kg<sup>-1</sup>], i.e. 55.95 [%] of the nominal power consumption is wasted.

As the intensity of the pressure pulse increases, that is the shock phenomenon, there is a gradual increase in instantaneous power consumption of the simulated screw compressor. However, this increase is by no means linear, but occurs in the form of exponential growth with different pitch intensities for shock compression and shock expansion. This difference is caused by the unequal physical impact of shock phenomena on the working process of the simulated machine.

The next step of this research will be, besides practical measurement of shock phenomena, also an advanced form of the computational model, where there will be an effort to minimize or eliminate the impact of idealizations in order to obtain more accurate results.

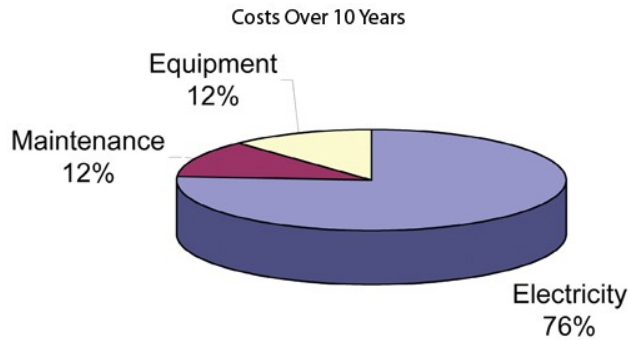
**Acknowledgement:** This article was written with the support of the following project: SP2019 / 156 – Research into specific areas of energy and environment.

## References

- [1] Kaminský Jaroslav, Kamil Kolarčík, Mojmír Vrtek, Možnosti úspor energie při výrobě, rozvodu a spotřebě stlačeného vzduchu v České republice, Prague: Technology Centre of the CAS, 2002, 31 p. ISBN 80-902689-3-5. <[https://www.tc.cz/files/istec\\_publications/moznosti-uspor-energie.pdf](https://www.tc.cz/files/istec_publications/moznosti-uspor-energie.pdf)>, (In Czech).
- [2] Furlong Ian, Tidal energy: "Why we should reap the benefits of being an island nation.", <<https://sites.google.com/site/ee535test/ian-furlong?tmpl=%2Fsystem%2Fapp%2Ftemplates%2Fprint%2F&showPrintDialog=1>>
- [3] Widell K. N., T. Eikevik, Reducing power consumption in multi-compressor refrigeration systems. International Journal of Refrigeration, Volume 33 (Issue 1), January 2010, pp. 88-94, DOI: 10.1016/j.ijrefrig.2009.08.006.
- [4] Marshall Ron, Design World – How to Calculate Compressed Air Savings, Compressed Air Challenge. <[https://www.designworldonline.com/how-to-calculate-compressed-air-savings/#\\_>](https://www.designworldonline.com/how-to-calculate-compressed-air-savings/#_>)
- [5] R. Keith Mobley, 14 - COMPRESSORS, Editor(s): R. Keith Mobley, Fluid Power Dynamics, Newnes, 2000, pp. 203-231, ISBN 9780750671743, <https://doi.org/10.1016/B978-075067174-3/50065-2>. (<http://www.sciencedirect.com/science/article/pii/B9780750671743500652>)
- [6] Kaminský Jaroslav, Kamil Kolarčík, Oto Pumpřla, Kompresory. (1st ed.), 2004, Ostrava: VŠB - Technical University of Ostrava,

- 122 p, ISBN 80-248-0704-1, (In Czech).
- [7] Mujic E., A. Kovacevic, N. Stosic, I. K. Smith, The influence of port shape on gas pulsations in a screw compressor discharge chamber, *Proceedings of the Institution of Mechanical Engineers, Part E: Journal of Process Mechanical Engineering*, Volume 222 (Issue 4), November 2008, pp. 211-223, DOI: 10.1243/09544089PME205
- [8] Baehr H. D., *Thermodynamik: Eine Einführung in die Grundlagen und ihre technischen Anwendungen*, 1966, Berlin / Heidelberg / New York: Springer-Verlag, 464 p., ISBN-10: 3642533574.
- [9] Noskiewič, J. et. Al, *Mechanika tekutin*, 1987, Prague: SNTL/ALFA, 354 p. (In Czech).
- [10] Dejč M. E., *Technická dynamika plynů – druhé vydání*, 1966, Prague: SNTL, 659 p, (In Czech).
- [11] Giampaolo T., *Compressor Handbook: Principles and Practice*, 2010, Lilburn: The Fairmont Press, 361 p., ISBN: 0-88173-616-3.
- [12] La plante R. Jeffrey, Rotary Screw Compression Process. In: *Gas Machinery Research Council Conference*, 2003, Salt Lake City, Utah. 9 p.
- [13] Wennemar Jurgen, et al, Dry Screw Compressor Performance and Application Range. In: *Proceedings of the 38th turbomachinery symposium*, 2009, Texas A&M University. Turbomachinery Laboratories, pp. 149–156.
- [14] Huang Paul Xiubao, Under-Compression (Over-Expansion) – An Isochoric or Adiabatic Process?, 2012, Purdue University, <<https://docs.lib.purdue.edu/cgi/viewcontent.cgi?referer=&httpsredir=1&article=3092&context=icec>>
- [15] Kaminský Jaroslav, *Využití pracovního prostoru pístových kompresorů*. (1st ed.), 1982 Prague: SNTL, 232 p, ISBN 80-248-0704-1, (In Czech).
- [16] P. X. Huang, S. Yonkers, D. Hokey, D. Olenick, “Screw pulsation generation and control: a shock tube mechanism,”. In: *Proceedings of the 8th International Conference on Compressors and Their Systems*, September 2013, London, UK, pp. 113–128.
- [17] H. Wu, Z. Xing, X. Peng, P. Shu, “Simulation of discharge pressure pulsation within twin screw compressors,” *Proceedings of the Institution of Mechanical Engineers, Part A: Journal of Power and Energy*, vol. 218, no. 4, 2004, pp. 257–264.
- [18] E. Mujic, A. Kovacevic, N. Stosic, I. K. Smith, “The influence of port shape on gas pulsations in a screw compressor discharge chamber,” *Proceedings of the Institution of Mechanical Engineers, Part E*, vol. 222, 2008, no. 4, pp. 211–223.
- [19] KONKA Karl-Heinz, *Schraubenkompressoren: Technik und Praxis*, 1988, Düsseldorf: VDI-Verlag, 500 p., ISBN 3-18-400819-3.
- [20] BAEHR H. D., *Thermodynamik: Eine Einführung in die Grundlagen und ihre technischen Anwendungen*, 1966, Berlin / Heidelberg / New York: Springer-Verlag, 464 p., ISBN-10: 3642533574.
- [21] NOŽIČKA Jiří, *Mechanika tekutin*, 2004, Prague: Publisher ČVUT, ISBN 80-01-02865-8, (In Czech).
- [22] HEJZLAR R., *Termodynamika* (4th ed), 2004, Prague: Publisher ČVUT. ISBN 80-01-02975-1.
- [23] NETRVAL Lukáš, *Návod na obsluhu a údržbu pro šroubový kompresor, AM 18 B1 / AM 22 B1 / AM 30 B1*. AM 18-8 B1. <<https://docplayer.cz/369863-Navod-na-obsluhu-a-udrzbu-pro-sroubovy-kompresor-am-18-b1-am-22-b1-am-30-b1-am-18-8-b1-obj-cislo-h-417-508-am-18-10-b1-obj.html>>, (In Czech).
- [24] KADLEC Zdeněk, *Termomechanika: návody do cvičení* (2nd ed.), 2008, Ostrava: VŠB - Technical University of Ostrava, ISBN 978-80-248-1736-1, (In Czech).
- [25] *Strojirenstvi.studentske.cz*, 14. Řemenové převody, <<http://strojirenstvi.studentske.cz/2010/11/14-remenove-prevody.html>>, (In Czech).
- [26] Pitzer Kenneth S., et al., *Molecular Structure and Statistical Thermodynamics: Selected Papers of Kenneth S Pitzer*, 1993, Singapore; River Edge, NJ: World Scientific, 536 p., ISBN: 978-981-4503-98-3.
- [27] Holeček Miroslav, *Termomechanika 4. Přednáška*, <<https://docplayer.cz/113624595-Termomechanika-4-prednaska.html>>, (In Czech).
- [28] Moran J., Michael, Howard N. Shapiro, *Fundamentals of Engineering Thermodynamics – 5th Edition*, 2006, New York: John Wiley & Sons, 831 p., ISBN 13 978-0-470-03037-0.
- [29] Kaminský Jaroslav, Kamil kolarčík, Mojmír Vrtek, *Provoz šroubových kompresorů – internal teaching texts*, 2002, Ostrava: VŠB - Technical University of Ostrava, 30 p., Not published, (In Czech).
- [30] Bloch P. Heinz, *A Practical Guide to Compressor Technology – Second Edition*, 2006, New Jersey: John Wiley & Sons 555 p., ISBN: 978-0-471-72793-4.
- [31] Zhao B., S. Han, L. Xu, C. Shi, D. Gao, Y. Zhang, Study on heat transfer of leakage flow in tooth tip clearance for single screw compressor based on fuzzy contoured finite element method. *Numerical Heat Transfer; Part A: Applications*, vol. 72, issue 7, 2017, pp. 551-562, DOI: 10.1080/10407782.2017.1386511.
- [32] Kolarčík Kamil, Jaroslav Kaminský, Jiří Nezhoda, *Metodika popisu polytropické stavové změny a výpočtu polytropické účinnosti u kompresorů*, 2014, Ostrava: VŠB - TU Ostrava, <[https://obd.vsb.cz/fcgi/verso.fpl?fname=obd\\_public\\_det&id=286078298](https://obd.vsb.cz/fcgi/verso.fpl?fname=obd_public_det&id=286078298)>, (In Czech).
- [33] Bogdanovska Gabriela, Vierošlav Molnar, Gabriel Fedorko, Failure analysis of condensing units for refrigerators with refrigerant R134a, R404A, *International Journal of Refrigeration-Revue Internationale du Froid* Volume: 100, Published: APR 2019, Pages: 208-219.

## Appendix A: Operating costs of a decade of typical air compressor operation [4]



## Appendix B: Energy characteristics of simulated screw compressor in comparison with energy characteristics of screw compressors from practical measurements

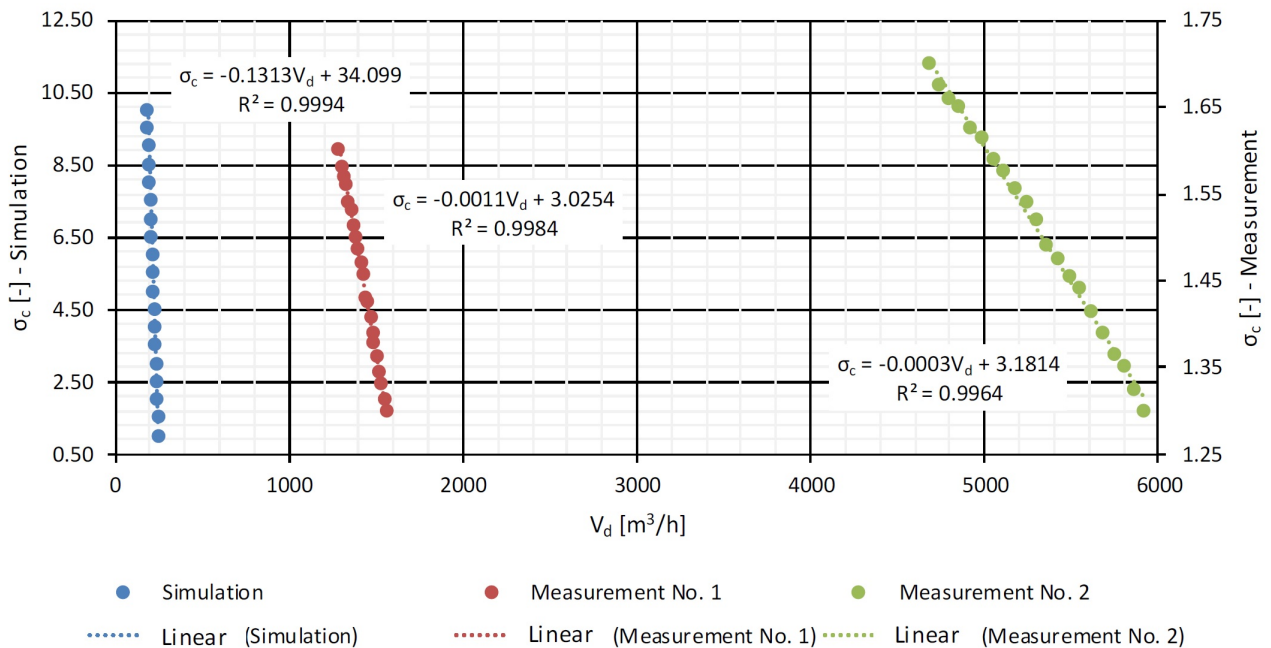


Figure B1: Pressure characteristics

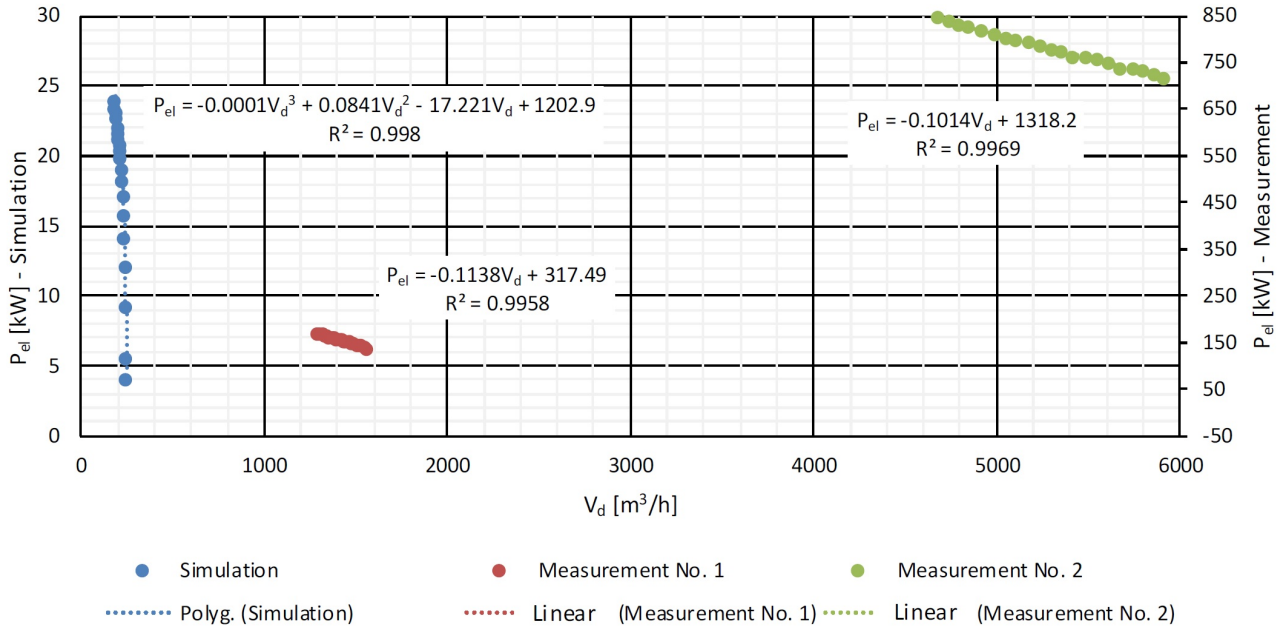


Figure B2: Power consumption characteristics

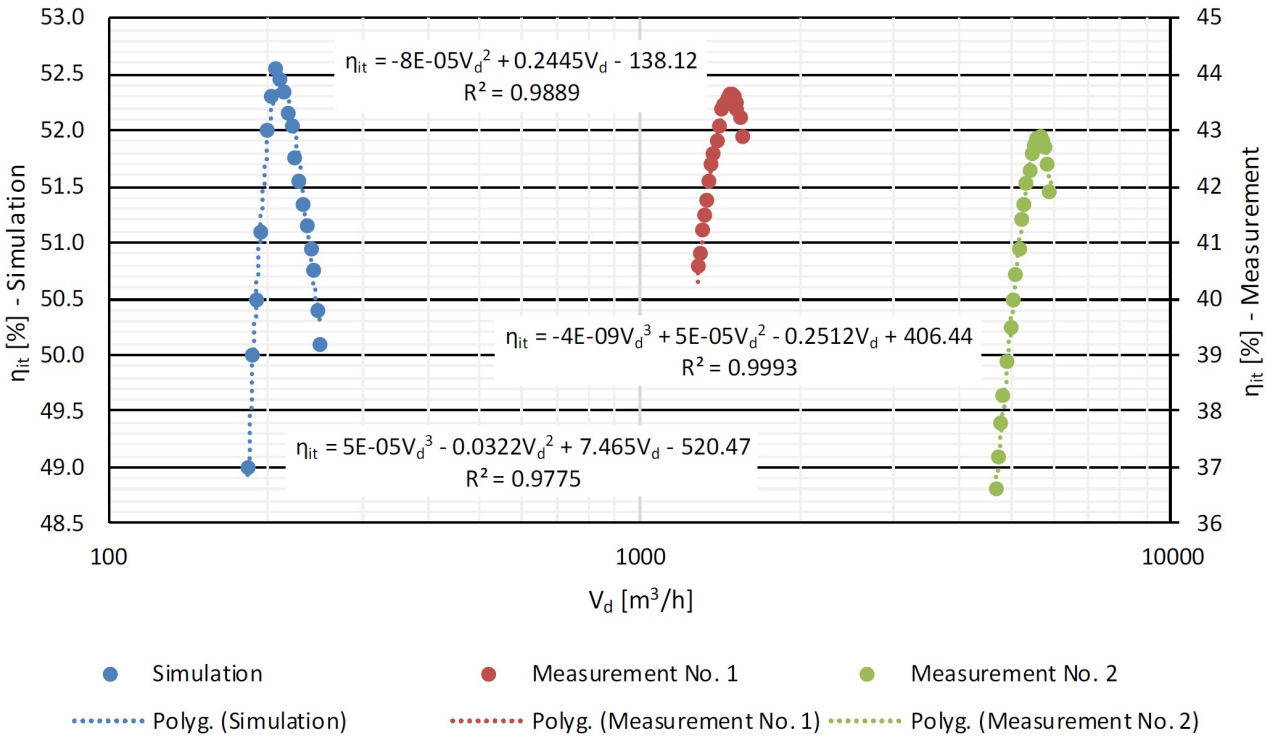


Figure B3: Efficiency characteristics



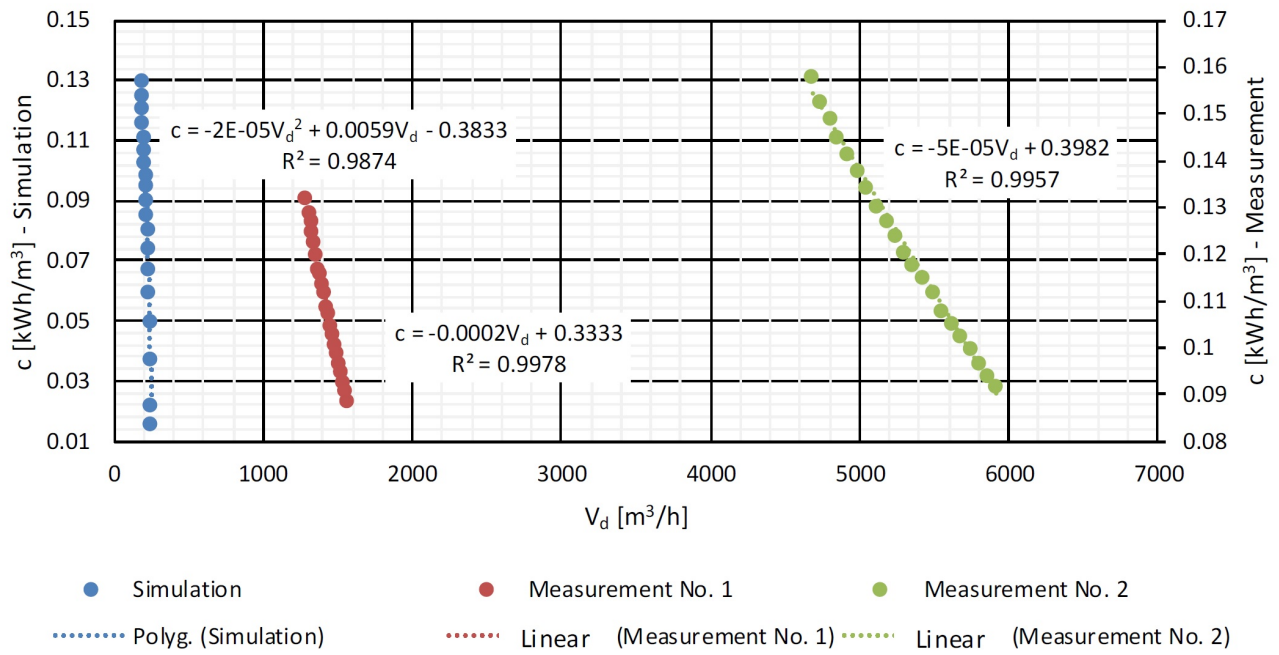


Figure B4: Specific energy consumption characteristics